PNAS
www.pnas.org

Supplementary Information for

Two Polymorphic Cholesterol Monohydrate Crystal Structures Form in Macrophage-derived Foam Cells. Relevance to Atherosclerosis

Neta Varsano[1], Fabio Beghi[2], Nadav Elad[3], Eva Pereiro[4], Tali Dadosh[3], Iddo Pinkas[3], Ana J Perez-Berna[4], Xueting Jin[5], Howard S. Kruth[5], Leslie Leiserowitz6, and Lia Addadi*[1]

Paste corresponding author name here
Email: Lia.Addadi@weizmann.ac.il

This PDF file includes:

Supplementary text
Figs. S1 to S9
References for SI reference citations

Supplementary Information Text

Supplemental Materials

DMEM culture medium was obtained from Gibco (Grand Island, NY, USA). 35 mm Dishes and No. 1.5 Coverslips, Glass 14 mm Diameter, uncoated (Cat# P35G-1.5-14-C), were obtained from MatTek Corporation (Ashland, MA, USA). QUANTIFOIL® R 2/2 on Au G200F1 200 mesh finder grids with holey carbon or SiO2 support film were obtained from Quantifoil Micro Tools (Jena, Germany). Acetylated LDL (acLDL) (Cat# BT-906) was obtained from Alfa Aesar (Heysham, UK). Alexa Fluor® 115-605-020 647-AffiniPure Goat Anti-Mouse IgM, μ-Chain Specific (Cat# 115-605-020), was obtained from Jackson ImmunoResearch (West Grove, PA, USA). Dulbecco's phosphate-buffered saline (DPBS) with Ca 2+ and Mg 2+ (Cat# 02-020-1A) were obtained from Biological Industries (Kibbutz Beit-Haemek, Israel). Bovine Serum Albumin (Cat# A9647), Fetal Bovine Serum, Gold nanoparticle suspension (with 150 nm diameter, Cat# 742058) and cholesterol carrier methyl-β-cyclodextrin (MβCD) (Cat# C-4555) were obtained from Sigma- Aldrich (St Louis, Missouri, MO).

Cholesterol monohydrate (Cat# 700000P), DPPC (Cat# 850355P) POPC (Cat# 850457C) and polycarbonate membrane with a pore diameter of 0.1 μm, were obtained from Avanti Polar (Avanti Polar Lipids, Birmingham, AL). Cholesterol was recrystallized before use for each experiment following a well-established protocol (1). The pure crystals were filtered and kept at −20 °C under a nitrogen atmosphere. Lipids were used without further purification, and kept at 10−3 M stock solutions in chloroform at −20°C until use.

Supplemental Methods

Antibody Purification

The monoclonal 58B1 antibodies were purified from the supernatant hybridoma fluid by affinity chromatography using an ImmunoPure IgM purification kit according to the manufacturer's instructions. The purified fractions were checked by UV absorbance at 280 nm, and those with optical density higher than 0.2 were collected and dialyzed (Spectra/Por membrane with cutoff 12000−14000 Da) in 2 L of phosphate-buffered saline (PBS) at 4 °C (the PBS solution was changed three times every 4 h). The antibodies were used for a maximum of 5 days after purification. The antibody concentration was checked by UV absorbance at 280 nm each day before use.

Cell culture

Murine macrophage-like J774A.1 cells were obtained from the American Type Culture Collection (ATCC; Manassas, VA, USA), and were cultured in DMEM (Dulbecco's

modified Eagle's medium, Gibco), supplemented with 10% fetal calf serum (FCS), 100 units/ml penicillin, 100 g/ml streptomycin and 1% L-glutamine. Cultures were maintained in a water-saturated atmosphere of 5% CO2. Uptake of acLDL particles followed the reported protocol (2).

Immunolabeling

Cells were cultured on glass bottom culture dishes or on gold TEM quantifoil grids, at a seeding density of 10^5 cells/cm^2. The cells were incubated with or without 50 µg/ml acLDL for different time lengths in serum depleted media. After incubation, the cells were rinsed three times in PBS and with 4% paraformaldehyde (PFA), 0.1% glutaraldehyde (GA) in PBS at room temperature for 1 hour, and excess fixative was removed with three washes in PBS containing 0.1% bovine serum albumin (BSA). Cells were incubated 60 min with 3 µg/ml purified MAb 58B1 IgM diluted in PBS containing 0.1% BSA. After three rinses in PBS (5 min each), cultures were incubated 30 min with 0.4 µg/ml Alexa Fluor 647 Goat Anti-Mouse IgM secondary antibody diluted in PBS containing 0.1% BSA. Cultures were rinsed three times with PBS containing 0.1% BSA and observed on the same day. Control cultures were incubated without acLDL or incubated with acLDL but stained only with secondary antibody and were measured in parallel to the sample under the same experimental conditions.

STORM imaging

Three dimensional super-resolution images were recorded with Vutara SR 200 (Bruker) commercial microscope based on the single-molecule localization 3D Biplane approach. Cholesterol crystals labeled with AlexaFluor 647 were imaged using 647 nm excitation laser and 405 nm activation laser in an imaging buffer composed of 5 mM cysteamine, oxygen scavengers (7 µM glucose oxidase and 56 nM catalase) in 50 mM Tris with 10 mM NaCl and 10% glucose at pH 8.0. Images were recorded using a 60x, NA 1.2 water immersion objective (Olympus) and Evolve 512 EMCCD camera (Photometrics) with gain 50, frame rate 50 Hz, and maximal power of 647 and 405 nm lasers set at 6 and 0.05 kW/cm^2, respectively.

Signal was recorded from the entire volume of the cell in multiple *z*-positions using 0.5 µm or 1 µm steps. At each *z* position, 2000 frames are acquired at 50 Hz. The maximum image resolution is 20 nm laterally (*x* and *y*) and 40-50 nm axially (in *z*).

The cholesterol domains size was determined using the Cluster Analysis Module of the Vutara SRX statistical software (version 6.01.12). This Module is an "Image-Based" cluster identification algorithm designed to generate grouped clusters of localizations within the context of the larger data set. The cluster analysis algorithm creates a binary image of the localization data by effectively binning the localization data. It then finds connected components in the binary image in the projected three-dimensional data set and use those connected regions to correlate where the overall clusters within the data are located. The parameters used in the analysis are: particle size of 50 nm, a minimum of 20

particle counts per cluster, opacity of 0.6, and accumulation threshold (to distinguish clusters from background in the density map) of 0.05.

Cryo-soft X-ray tomography

For 3D imaging of the cell and associated cholesterol crystals we used cryo-SXT with the 40 nm zone plate lens at 520 eV, which has a measured depth of field (DOF) of 3.3 μm (3). Gold quantifoil TEM *finder* grids were glow-discharged and sterilized under UV light for 30 min. Cells were cultured on the grids and incubated with or without acLDL for different time lengths, fixed and labeled as described above. The specimens were observed on the same day in the VUTARA SR200 system described above. Fixed cells were then kept in PBS at 4^{o}C overnight and vitrified the next day by plunging into liquid ethane.

Grids are lifted by tweezers and held in the plunger chamber at 90% relative humidity and 22 ^{o}C (Leica EM-GP plunger, Leica Microsystems). A drop of 3 mL gold nanoparticle suspension (150 nm) is placed on top of the grid and blotted for 3 s. Grids are then plunge-frozen in liquid ethane. Frozen samples are mounted on a cryogenically cooled sample holder at the MISTRAL beamline, ALBA synchrotron, Barcelona, Spain (4, 5).

The soft X-ray projection single-tilt series were collected from a number of locations on several grids at X-ray energy of 520 eV.

For a multifocal tomogram, data were obtained by combining several tilt series, which were taken at different focal planes following the XTEND procedure for extending the depth of field in cryo soft X-ray tomography (6).

Parameters relative to figures in the main text. Figure 1: 3 focal series were acquired using steps of 5.3 μm suitable for ~8 μm thick cells (6). Tomograms were taken in the range of [−60°, 70°] with steps of one degree, using one-second exposure time and 15 nm pixel size. Figure 2: Tomogram was taken in the range of [−60°, 70°] using 1-degree steps, with one-second exposure time. Pixel size: 15 nm. Figure 4 and Figure 6F: Figure 4 is composed of a mosaic of three reconstructed tomograms. The tomograms at the right and left of the figure were taken in the range of [−65°, 65°] using 1-degree steps, with one-second exposure time and 13 nm pixel size. Segmented crystal from the left tomogram is shown also in Figure 6F. The tomogram in the middle of the figure is a multi-focal tomogram: 3 focal series were acquired using steps of 5.3 μm suitable for ~8 μm thick cells (6). Tomograms were taken in the range of [−60°, 65°] using 1-degree steps, with one-second exposure time and 13 nm pixel size.

Figure 6 (C-D): Tomograms were taken in the range of [−65°, 40°] using 1-degree steps, with one-second exposure time. Pixel size: 13 nm. Figure 6E: Tomogram was taken in the range of [−65°, 65°] using 1-degree steps, with one-second exposure time. Pixel size: 13 nm.

Figure S4: Tomogram was taken in the range of [−60°, 65°] using 1-degree steps. Exposure times were varied from 5 to 3 seconds, depending on the tilt angle. Pixel size: 15 nm.

The alignment of the tomographic projections was performed in bsoft (7) using gold nanoparticles and/or lipid-rich cellular organelles as fiducial markers. The aligned projection tilt series were reconstructed using tomo3d (8, 9).

Correlative cryo-SXT/STORM

Overlay of the data was performed following the guidelines previously described (10). For alignment in *xy*, light microscopy and STORM images of Alexa-647 signal were overlaid onto images from the X-ray mosaic projection scans and the reconstructed data. 3D STORM localization map of the entire cell volume was then rotated in *xy* accordingly. For the alignment in *z*, the relevant features that were imaged by the X-rays (nucleus, plasma membrane and lipid bodies) were first segmented based on their contrast and rendered in 3D using Avizo® software. The 3D STORM signal, which was taken from the entire volume of the cell, was then super-imposed on the segmented X-ray volume following the outline of the plasma membrane of the cell. Each of the data sets were sliced into layers of 150 nm and loaded into the tailor-made Correlator script (10). Following loading, the software overlays the data for every possible *z*-shift. The output is a graph which quantifies the percentage of the super resolution signal coming from the cell area for every given *z* shift, relative to the overall STORM signals in all slices. The optimal *z* position is chosen where most of the super-resolution signals are located within the cell (Fig. S9).

For cases when the STORM signal was taken from a few micrometers large structures (that can be easily recognized by STORM and X-ray imaging), the height of the structure from the foil was recorded and was used for the superimposition (Fig. S1).

Raman spectroscopy

Cells were cultured on glass bottom culture dishes, at a seeding density of 10^5 cells/cm^2. Then, the cells were incubated with acLDL for 36hr as described above. Cells were rinsed three times in PBS and fixed by incubating with 4% PFA, 0.1% GA in PBS at room temperature for 1 hour. Additional three washes in PBS were performed to remove any excess of fixative and the cells were left under PBS throughout the experiment.

Anhydrous cholesterol crystals (Fig. S5) were obtained by adding 0.3gr cholesterol powder to 10mL of boiling acetone. The solution was cooled to room temperature, filtered and the filtrate was left at 4 °C for 3 days. The crystals were filtered and kept at −20 °C under a nitrogen atmosphere. Crystals were characterized by X-ray powder diffraction (Fig. S5II).

Triclinic cholesterol monohydrate was recrystallized as described (1) and measured under water to prevent dehydration.

Raman measurements were conducted on a LabRAM HR Evolution instrument (Horiba, France) configured with four laser lines (325, 532, 632, and 785 nm), allowing for Raman spectra from 50 cm^{-1} and onward. The instrument is equipped with an 800 mm spectrograph. The system's pixel spacing is 1.3 cm^{-1} when working with a 600 grooves/mm grating at 632 nm excitation. The sample is exposed to light by various objectives (MPlanFL N NA-0.9, 100X, LUMPLFLN NA-1.0 60XW, and LMPlanFL N

NA-0.5 50X LWD, Olympus, Japan). The LabRAM instrument is equipped with a CCD detector: a 1024 × 256 pixel open electrode front illuminated CCD camera cooled to −60 °C. The system is set around an open confocal microscope (BX-FM Olympus, Japan) with a spatial resolution of about 1 μm using the 60X WI objective. The data analyses presented in this research was performed for the most part using the 632 nm HeNe laser, the 600 grooves/mm grating, and the 60X WI objective.

Preparation of Supported Lipid Bilayers

Supported lipid bilayers were prepared following the vesicle fusion procedure (11, 12). To deposit the hydrophilic "cushion" for the bilayer, gold 200 mesh TEM grids, coated with SiO_2 2/2 quantifoil were glow-discharged for 2 min and then immediately immersed in solutions of 1000 ppm PEI for 20 min (13).

Vesicles with the desired lipid ratios of 42:18:40 mol% Cholesterol/DPPC/POPC were prepared following a previously described procedure (12), Briefly, 0.14 mg of the desired lipid mixture was prepared by mixing the appropriate amounts of lipid dissolved in chloroform. The mixture was dried and kept under vacuum for at least 15 min, and then hydrated with 1 mL of Milli-Qgrade water. The suspension was heated above the lipid transition temperature 75 ºC and mixed by vortex 3 times (3 min each), followed by five additional cycles of freezing and heating the mixture above 75 ºC (5 min each). The suspension was extruded nine times through a polycarbonate membrane with a pore diameter of 0.1 μm (Avanti Polar Lipids) at 75 °C. Vesicle suspensions were spread on the hydrophilic grid-surface such that the final lipid concentration was 0.14 mg/mL in DDW. The sample was heated to 75 ºC for 15−20 min to allow the spontaneous process of vesicle adhesion, fusion, and rupture to take place on the surface. The samples were washed three times with DDW to remove unruptured vesicles.

Cryo-TEM for Electron Diffraction

Cell samples: carbon-coated gold Quantifoil TEM *finder* grids were glow-discharged and sterilized under UV light for 30 min. Cells were cultured on the grids and incubated with acLDL for 48hr and 36hr as described above. At the end of the incubation time the grids were plunge frozen into liquid ethane cooled by liquid nitrogen, using a Leica EM-GP plunger. The plunger chamber was maintained at 90% humidity and 37 ˚C and blotting time was 5sec. Samples were maintained at liquid nitrogen temperature in the TEM using a Gatan 626 cryo-holder.

Lipid-Bilayer samples: Following the preparation of supported lipid bilayers on grids, the samples were incubated with the cholesterol delivery system as described (12). Briefly, a saturated solution of cholesterol in chloroform (60 μL) was injected into 4 mL of MβCD:cholesterol water solution. The grids with the deposited lipid bilayer were placed inside designated box with suitable wells. At the end of the incubation, the grids were washed with DDW, blotted, and immediately plunge-frozen into liquid ethane as described above. The plunger chamber was maintained at 20 ˚C with 90% humidity and blotting time

was 3.5sec. Samples were maintained at liquid nitrogen temperature in the TEM using a Gatan 626 cryoholder.

For figure 5A: images and diffraction patterns were recorded using an FEI Tecnai F-20 TEM operating at 200 kV and equipped with a Gatan US4000 CCD camera, under low dose conditions.

For figure 5B, C and Fig 6A: Images and diffraction patterns were recorded using an FEI Tecnai T-12 TEM operating at 120 kV on a Gatan OneView camera.

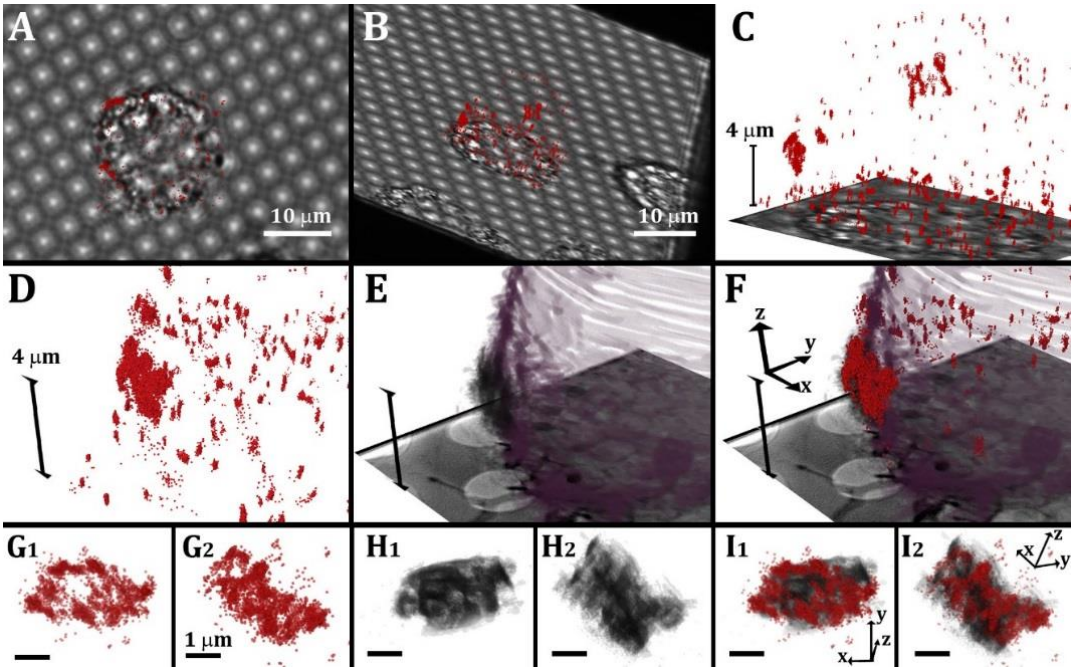

Fig. S1 Alignment of STORM/cryo-SXT in *z* for micron-size labelled crystals.
(A-C) Bright field image from wide field (A and B) or EMCCD (C) cameras. Images show a J774A.1 cell following incubation with acLDL, fixation and antibody 58B1 labelling, overlaid with the corresponding STORM data (red), viewed from top (A) or side views (B and C) . *(D)* STORM localization map loaded to Avizo® software. *(E)* 3D SXT segmented data from a side view. The different features are segmented using arbitrary colors: plasma membrane (purple), cholesterol crystal (black-grey). *(F)* Superimposition of D and E. *(G1 and G2)* STORM localization map of the micron-labeled aggregate from different orientations. *(H1 and H2)* The corresponding segmented SXT data of (G1 and G2) respectively. *(I1 and I2)* Superimposition of H and G. The cell is the same in figure 2. The aggregate is the same as in figure 2 *D-G*, in different orientations.

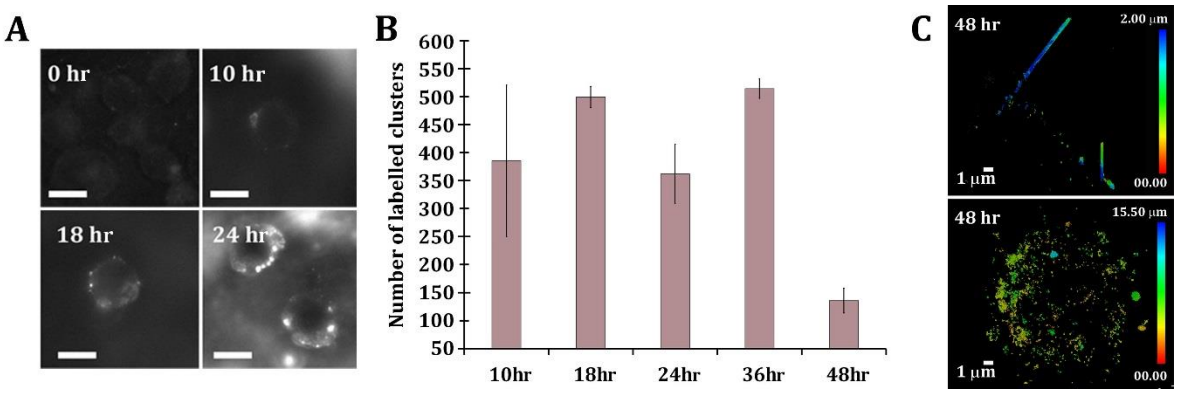

Fig. S2 Time evolution of plasma membrane crystalline cholesterol domains in macrophage J774A.1 cells *(A)* Wide field fluorescence micrographs of cells incubated with acLDL for different times. Scale bar=10µm. *(B)* STORM cluster count after different incubation times. Data are shown as the average count of clusters in different cells (n=3-6) ± standard error. Data were analyzed using the Cluster Analysis Module of the Vutara SRX statistical software (version 6.01.12). *(C)* Resolved super-resolution localization map after incubation times with acLDL for 48hr. The color scales indicate the heights of the domains in the cell: blue, top of the cell, red, bottom of the cell.

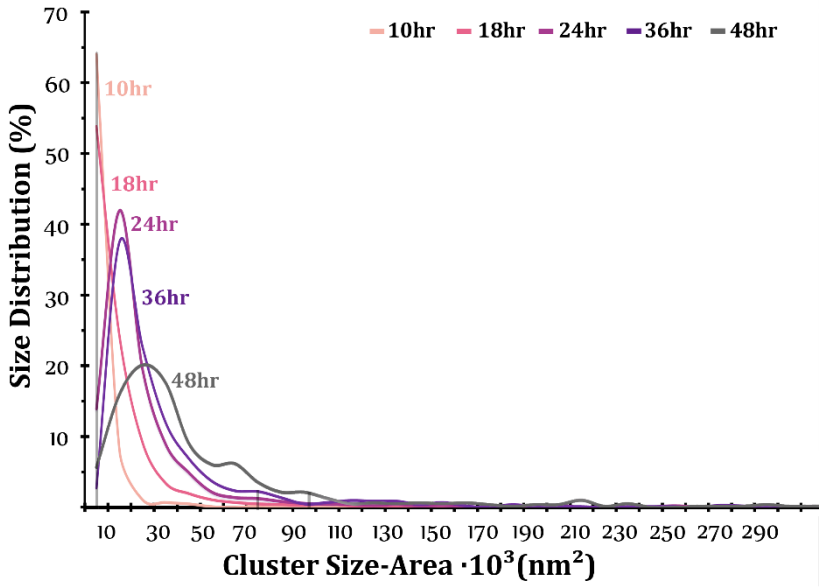

Fig. S3 Distribution of segregated cholesterol-cluster sizes in macrophage cells after different incubation times with acLDL. Data were analyzed using Vutara SRX statistical package as described in the methods above. Cluster size area was determined for clusters with >20 particles. After 24 hours of incubation, only 15% of the cluster populations are 30-100 nm, corresponding to 1-10·10^3 nm^2 in the figure (onset of the curves, grey line), and they further decrease to 5% after 48 hours of incubation.

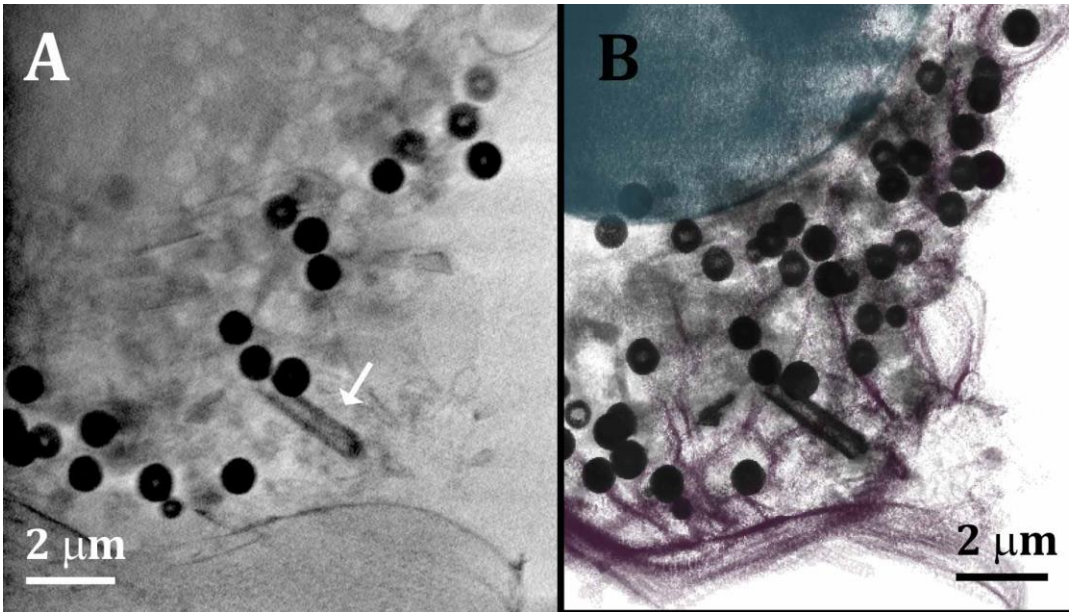

Fig. S4 Cryo-SXT of tubular cholesterol crystal grown by a cell. *(A) z* projection of 180 SXT slices of the reconstructed cell tomogram. *(B)* Whole cell volume 3D SXT segmented data of the same cell as in A. The different features are segmented using arbitrary colors: plasma membrane (purple), cholesterol crystal and lipid bodies (black-grey), cell nucleus (blue).

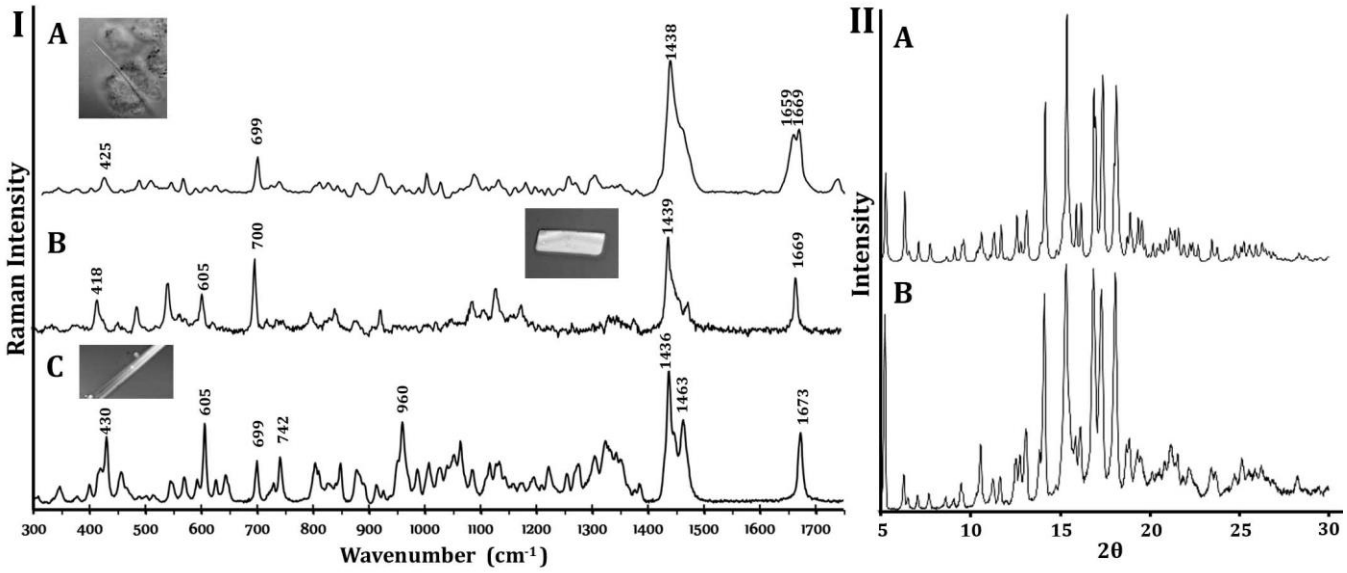

Fig. S5 *(I)* Micro-Raman spectra of: *(A)* Intracellular cholesterol crystal formed within a J774A.1 cell. The measurement was carried out with the laser illuminating a point on the crystal outside of the cell; (*B)* Cholesterol monohydrate triclinic crystal (in water); *(C)* Anhydrous cholesterol crystal. The peaks at 430 cm^{-1}, 742 cm^{-1}, 960cm^{-1} and 1673 cm^{-1} are characteristic of anhydrous cholesterol and are absent in the cell-grown crystal and in the cholesterol monohydrate crystal. In the cell grown crystal, the group of peaks between 1400–1500 cm^{-1} is also markedly similar to that of cholesterol monohydrate, and not to anhydrous cholesterol. (*II)* X-ray powder diffraction of anhydrous cholesterol. *(A)* Simulated diffraction pattern of anhydrous cholesterol from reported structure (14). *(B)* Anhydrous cholesterol recrystallized from acetone and measured by Raman in IC.

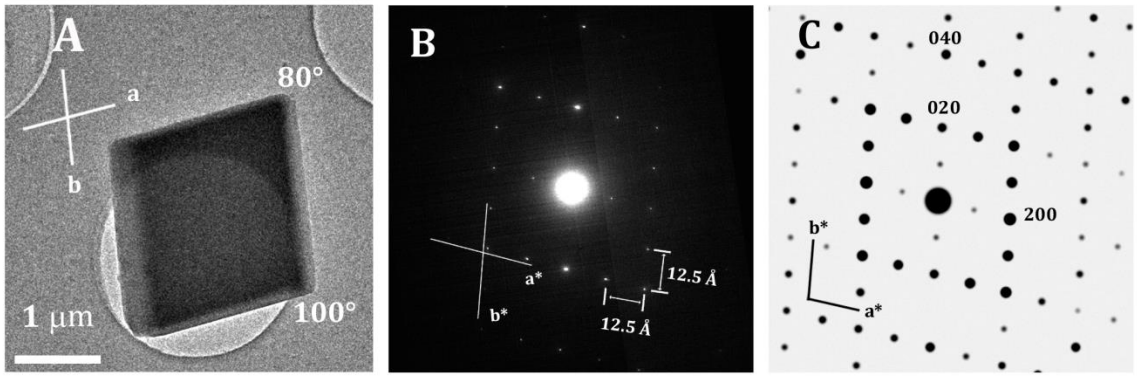

Fig. S6 Cryo-TEM image and diffraction of a triclinic cholesterol monohydrate crystal. The crystal was grown on a supported lipid bilayer composed of cholesterol/DPPC/POPC= 42/18/40 mol% externally supplemented with cholesterol. *(A)* Transmission electron micrograph of the crystal with its crystallographic axes. *(B)* Electron diffraction pattern of the crystal in A. (*C)* simulated electron diffraction pattern obtained from the triclinic structure, in direction [001]. The diffraction shows $P\bar{1}$ symmetry.

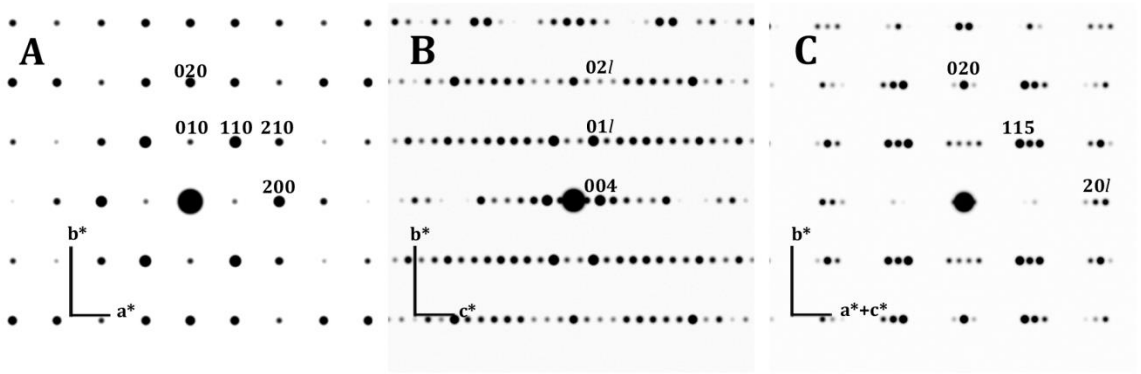

Fig. S7 Simulated electron diffraction pattern of the cholesterol monohydrate monoclinic polymorph, showing Laue mm symmetry. *(A)* Projected along the [001] direction. *(B)* Projected along the [100] direction. *(C)* Projected along the [101] direction; because of the length of the *c* axis, *c** is short, causing more reflections to appear simultaneously as satellites.

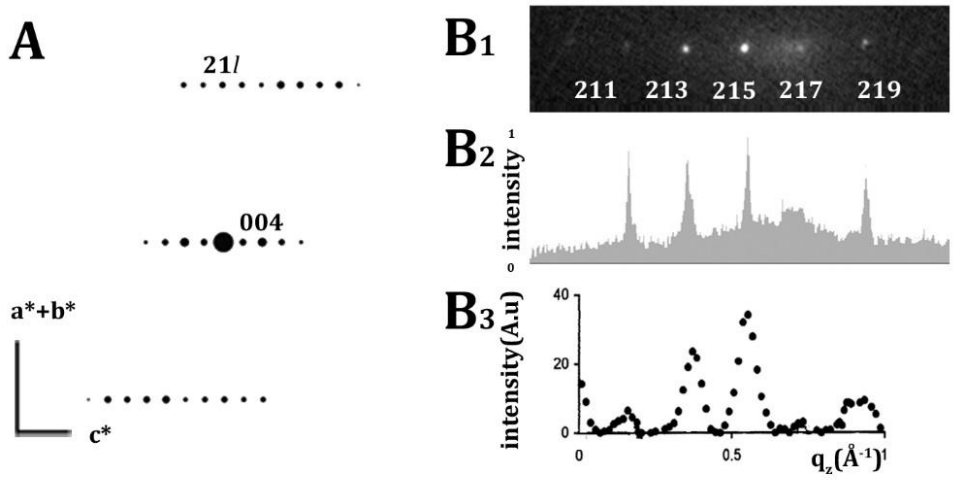

Fig. S8 Intensity profile of 21*l* diffractions of the monoclinic polymorph of cholesterol monohydrate. *(A)* Simulated electron diffraction pattern of cholesterol monohydrate monoclinic structure projected along the [$\bar{1}$20] direction, showing P$\bar{1}$ Laue symmetry. *(B_1)* High magnification of 21*l* diffracted spots taken from the intracellular crystal diffraction presented in Figure 5D4. *(B_2)* Normalized intensity profile of the diffracted spots presented in B_1; *(B_3)* Intensity profile of 21*l* spots measured from crystalline cholesterol multilayers by grazing X-ray diffraction. B_3 reprinted from ref. (15) with permission from Elsevier.

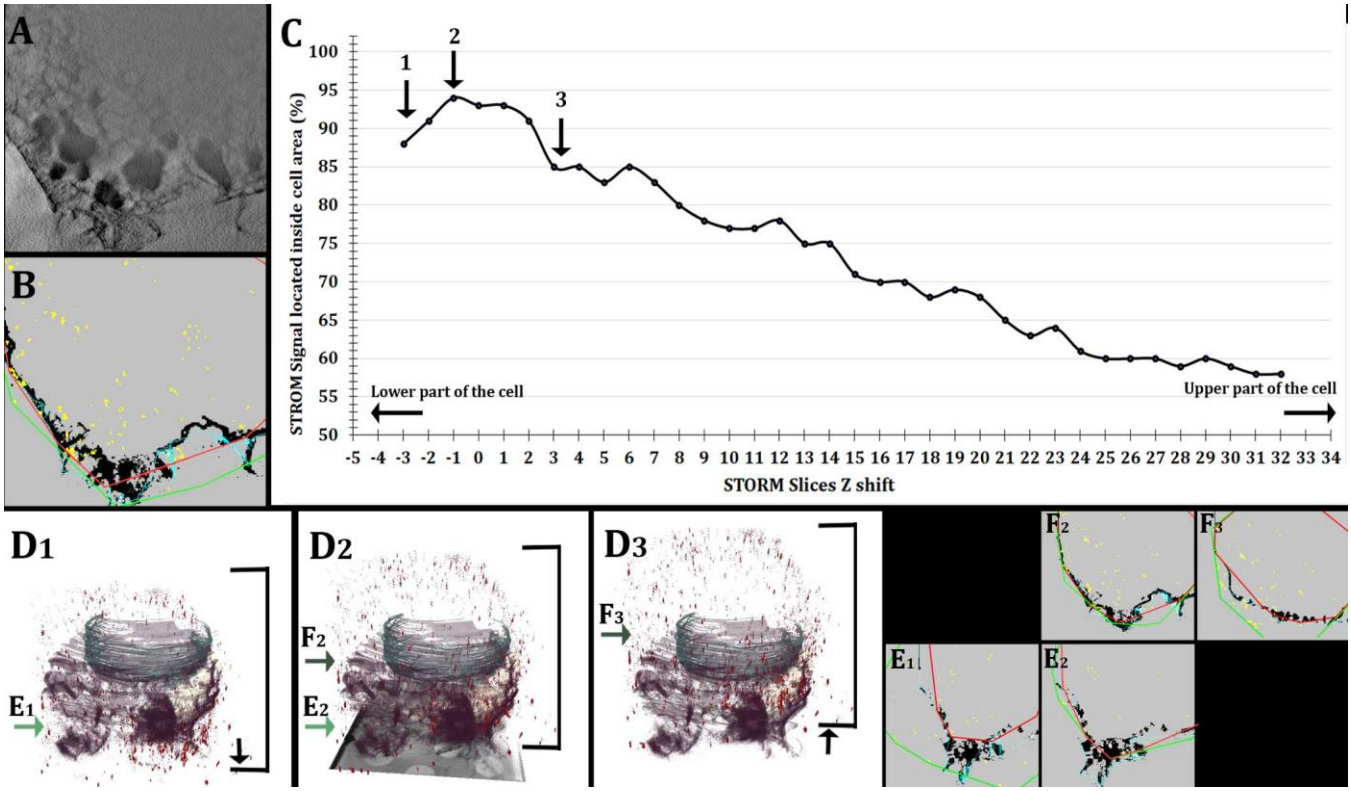

Fig. S9 Alignment of STORM/cryo-SXT in *z* using the tailor-made correlator. *(A)* A slice through the reconstructed X-ray data. The sliced segmented tomogram layers are loaded into the tailor-made Correlator script (10). *(B)* The script finds the cell contour (blue outline) based on the segmented contrast. The STORM sliced data (yellow dots) are loaded into the script and the spots are localized (green outline). STORM data are superimposed on the SXT data. The script calculates the percentage of STORM signal coming from the cell area for every given *z* shift. Namely, spots inside the cell (red outline) relative to spots inside the green outline (the total STORM signal). *(C)* Graphical output of the script presenting the percentage of the super resolution signal included inside the cell area for every *z* shift. *(D1-3)* 3D reconstructions of the cell that visually correspond to several *z* shift scenarios labeled 1 – 3 in C. The black brackets represent the STORM signal (red spots) as it slides relative to the segmented cell (black arrows). The green arrows point to the corresponding overlaid *z* shift positions in E and F. *(E, F)* Overlaid data for the different *z* shifts as indicated in D1-3. At low *z* shift (D1, E1) low percentage of STORM signal is located inside the cell. At high *z* shift (D3, F3) low percentage of STORM signal is located inside the cell. The alignment position is chosen where STORM signals is enveloped by the cell contour, with some signal superimposed to the plasma membrane (indicated as 2 in C, D2, E2 and F2). Different features are segmented based on contrast in arbitrary colors: plasma membrane: purple, nucleus: blue, lipid bodies: yellow).

References

1. Perl-Treves D, Kessler N, Izhaky D, & Addadi L (1996) Monoclonal antibody recognition of cholesterol monohydrate crystal faces. *Chem. Biol.* 3(7):567-577.
2. Ong DS*, et al.* (2010) Extracellular cholesterol-rich microdomains generated by human macrophages and their potential function in reverse cholesterol transport. *J. Lipid Res.* 51(8):2303-2313.
3. Otón J*, et al.* (2016) Characterization of transfer function, resolution and depth of field of a soft X-ray microscope applied to tomography enhancement by Wiener deconvolution. *Biomedical optics express* 7(12):5092-5103.
4. Pereiro E, Nicolas J, Ferrer S, & Howells M (2009) A soft X-ray beamline for transmission X-ray microscopy at ALBA. *J. Synchrotron Rad* 16(4):505-512.
5. Sorrentino A*, et al.* (2015) MISTRAL: a transmission soft X-ray microscopy beamline for cryo nano-tomography of biological samples and magnetic domains imaging. *J. Synchrotron Rad* 22(4):1112-1117.
6. Otón J*, et al.* (2017) XTEND: Extending the depth of field in cryo soft X-ray tomography. *Scientific Reports* 7.
7. Heymann JB, Cardone G, Winkler DC, & Steven AC (2008) Computational resources for cryo-electron tomography in Bsoft. *J. Struct. Biol.* 161(3):232-242.
8. Agulleiro J & Fernandez J-J (2011) Fast tomographic reconstruction on multicore computers. *Bioinformatics* 27(4):582-583.
9. Agulleiro J-I & Fernandez J-J (2015) Tomo3D 2.0–Exploitation of Advanced Vector eXtensions (AVX) for 3D reconstruction. *J. Struct. Biol.* 189(2):147-152.
10. Varsano N*, et al.* (2016) Development of Correlative Cryo-soft X-ray Tomography and Stochastic Reconstruction Microscopy. A Study of Cholesterol Crystal Early Formation in Cells. *J. Am. Chem. Soc.* 138(45):14931-14940.
11. Ziblat R, Fargion I, Leiserowitz L, & Addadi L (2012) Spontaneous formation of two-dimensional and three-dimensional cholesterol crystals in single hydrated lipid bilayers. *Biophys. J.* 103(2):255-264.
12. Varsano N, Fargion I, Wolf SG, Leiserowitz L, & Addadi L (2015) Formation of 3D cholesterol crystals from 2D nucleation sites in lipid bilayer membranes: implications for atherosclerosis. *J. Am. Chem. Soc.* 137(4):1601-1607.
13. Wong JY*, et al.* (1999) Polymer-cushioned bilayers. I. A structural study of various preparation methods using neutron reflectometry. *Biophys. J.* 77(3):1445-1457.
14. Shieh H, Hoard L, & Nordman C (1977) Crystal structure of anhydrous cholesterol. *Nature* 267(5608):287
15. Solomonov I, Weygand MJ, Kjaer K, Rapaport H, & Leiserowitz L (2005) Trapping crystal nucleation of cholesterol monohydrate: relevance to pathological crystallization. *Biophys. J.* 88(3):1809-1817.